



## Original Article

# Investigations on mechanical properties of aluminum hybrid composites

Dora Siva Prasad<sup>a,\*</sup>, Chintada Shoba<sup>b</sup>, Nallu Ramanaiah<sup>c</sup>

<sup>a</sup> Department of Mechanical Engineering, GITAM University, Visakhapatnam, India

<sup>b</sup> Department of Industrial Engineering, GITAM University, India

<sup>c</sup> Department of Mechanical Engineering, Andhra University, India

### ARTICLE INFO

#### Article history:

Received 25 June 2013

Accepted 26 November 2013

Available online 17 January 2014

#### Keywords:

Hybrid composites

Rice husk ash

Dislocation density

Double stir casting process

### ABSTRACT

A double stir casting process was used to fabricate aluminum composites reinforced with various volume fractions of 2, 4, 6, and 8 wt% RHA and SiC particulates in equal proportions. Properties such as hardness, density, porosity and mechanical behavior of the unreinforced and Al/x%RHA/x%SiC ( $x = 2, 4, 6,$  and  $8$  wt%) reinforced hybrid composites were examined. Scanning electron microscope (model JSM-6610LV) was used to study the microstructural characterization of the composites. It was observed that the hardness and porosity of the hybrid composite increased with increasing reinforcement volume fraction and density decreased with increasing particle content. It was also observed that the UTS and yield strength increase with an increase in the percent weight fraction of the reinforcement particles, whereas elongation decreases with the increase in reinforcement. The increase in strength of the hybrid composites is probably due to the increase in dislocation density. A systematic study of the base alloy and composites was done using the Brinell hardness measurement and the corresponding age hardening curves were obtained. It was observed that in comparison to that of the base aluminum alloy, the precipitation kinetics of the composites were accelerated by adding the reinforcement. This effectively reduced the time for obtaining the maximum hardness by the aging heat treatment.

© 2013 Brazilian Metallurgical, Materials and Mining Association. Published by Elsevier Editora Ltda. Este é um artigo Open Access sob a licença de [CC BY-NC-ND](http://creativecommons.org/licenses/by-nc-nd/3.0/)

## 1. Introduction

Composite materials are a mixture or a combination of two or more constituents differing in form and/or material composition and that are essentially insoluble in each other. Both constituents maintain their identity as they do not dissolve or melt in each other, and act in such a way that a new material results whose properties are better than the sum of their constituents. The incorporation of several different

types of ceramic particulates into a single matrix has led to the development of hybrid composites. Also, using a hybrid composite that contains two or more types of particulates, the advantages of one type of particulates could complement to what is lacking in the other [1].

Nowadays, the use of agro/industrial wastes as a secondary reinforcement in the fabrication of composites is gaining more importance. The advantages of using these wastes are production of low cost by-products, reduction in the cost of aluminum products [2], readily available with less cost,

\* Corresponding author.

E-mail: [dorasivaprasad@gmail.com](mailto:dorasivaprasad@gmail.com) (D.S. Prasad).

2238-7854 © 2013 Brazilian Metallurgical, Materials and Mining Association. Published by Elsevier Editora Ltda.

Este é um artigo Open Access sob a licença de [CC BY-NC-ND](http://creativecommons.org/licenses/by-nc-nd/3.0/) <http://dx.doi.org/10.1016/j.jmrt.2013.11.002>

and often lower densities in comparison with most technical ceramics (boron carbide and alumina). Many researches have reported the potentials and limitations of the use of wastes as reinforcements [3,4]. Prasad and Krishna [5] reported that the tribological properties of low-cost composites developed with the use of rice husk ash (RHA) have been increased along with some increase in mechanical properties. Prasad [6] investigated the damping behavior of the composites with rice husk ash as reinforcement and the results indicate the increase in damping capacity with the increase in particulate content. The increase in damping capacity has been attributed to several mechanisms such as thermoelastic damping, intrinsic damping, and interfacial damping. Several authors studied different properties of hybrid composites with graphite as reinforcement. Suresha [7] studied wear characteristics of hybrid aluminum matrix composites reinforced with graphite and silicon carbide particulates and found that hybrid composites exhibit better mechanical properties and wear characteristics. Jinfeng Leng et al. [8] studied the machinability of SiC/Gr/Al hybrid composites and their results showed that the presence of flake graphite particle acted as solid lubrication and promoted chip formation during cutting, resulting in an improved machinability. Alaneme et al. [9] studied the characterization and mechanical behavior of RHA reinforced hybrid composites and concluded that RHA has great promise to serve as a complementing reinforcement for the development of low cost products. Rice husk ash contains a quality of high surface area silica, which has been purified by chemical leaching and fluidization furnace. Mishra et al. [10] discuss the method of preparation of silicon and its purification procedure with rice husk ash. Rodriguez de Sensale [11] studied the strength development of concrete with rice husk ash. RHA is a highly pozzolanic material. The non-crystalline silica and high specific surface area of the RHA are responsible for its high pozzolanic reactivity. In the present work, an attempt was made to fabricate aluminum hybrid composites with silicon carbide (SiC) and agro waste RHA as reinforcements. Properties such as density, porosity, aging, and mechanical behavior were investigated and the related mechanisms have been discussed and presented.

## 2. Materials and method

### 2.1. Matrix material

In the present study, A356.2 with the theoretic density of 2760 kg/m<sup>3</sup> was used as a matrix material. The chemical composition of the matrix material is given in Table 1. RHA particulates with an average size of 25 μm and SiC particulates with an average size of 35 μm were used as reinforcement materials. The chemical composition of RHA is given in Table 2. Magnesium was selected as a wetting agent to improve

**Table 1 – Chemical composition of A356.2 Al Alloy matrix.**

Si	Fe	Cu	Mn	Mg	Zn	Ni	Ti
6.5–7.5	0.15	0.03	0.10	0.4	0.07	0.05	0.1

wettability between the matrix and the reinforcements during production of the hybrid composites.

### 2.2. Pretreatment of RHA

Before incorporating the rice husk ash particulates into the molten metal, RHA was pretreated to RHA to free it from inorganic matter and carbonaceous material. The RHA particulates were thoroughly washed with water to remove the dust and dried at room temperature for 1 day. The rice husk was then heated to 200 °C for 1 h to remove the moisture. It was then heated to 600 °C for 12 h to remove the carbonaceous material. After this operation, its color changed from black to grayish white. The silica-rich ash, thus obtained, was used as a reinforcement material in the preparation of composites.

### 2.3. Preparation of hybrid composites

The aluminum alloy was charged into the graphite crucible and heated to 750 °C till the entire metal in the crucible was melted. The reinforcement particles RHA and SiC were preheated to 700–800 °C for 1 h before incorporation into the melt to remove moisture. After the molten metal was fully melted, degassing tablet was added to reduce the porosity. Simultaneously, 1% by weight magnesium was added to the melt to enhance the wettability between the matrix and the reinforcements. A stirrer made up of stainless steel was lowered into the melt slowly to stir the molten metal at a speed of 700 rpm. The speed of the stirrer can be controlled by means of a regulator provided on the furnace. The preheated SiC particles were added into the molten metal at a constant rate during the stirring. Stirring was continued for another 5–10 min even after the completion of particle feeding. After this stage the Al/SiC composite slurry was allowed to maintain at 700 °C for 10 min without stirring. The composite slurry was then heated to 750 °C and preheated RHA particulates were poured at a constant rate and the stirring was continued for 20 min. The mixture was poured into the mold (prepared for tensile test specimens) which was also preheated to 500 °C for 30 min to obtain uniform solidification. Using this double stir casting process, 2, 4, 6 and 8% by weight of equal proportions of RHA/SiC particle-reinforced hybrid composites were produced.

**Table 2 – Chemical composition of RHA.**

Constituent	Silica	Graphite	Calcium oxide	Magnesium oxide	Potassium oxide	Ferric oxide
%	90.23	4.77	1.58	0.53	0.39	0.21

## 2.4. Microstructural characterization

The microstructure of the hybrid composites was examined using an optical microscope (Model: Olympus), and a scanning electron microscope (SEM). JSM-6610LV scanning electron microscope equipped with energy dispersive X-ray analyser (EDX) was used to study microstructure of the hybrid composites. The samples of unreinforced and hybrid composites for SEM were cut from tensile specimens and ground by means of abrasive papers followed by rotating disk cloth polishing. Keller's reagent (95 ml water, 2.5 ml HNO<sub>3</sub>, 1.5 ml HCl, 1.0 ml HF), very popular general purpose reagent for Al and Al alloys, was used as an etching agent.

## 2.5. XRD characterization

X-ray diffraction patterns of the rice husk ash sample are taken using an Ultima IV X-ray diffractometer with CuK $\alpha$  radiation and Ni filter. The XRD analysis was carried out at a voltage of 40 kV and 30 mA current intensity.

## 2.6. Density and porosity measurements:

Density measurements were carried out on the base metal and reinforced samples using the Archimedes principle. This method of density measurement simply involves weighing the sample in air and in another fluid of known density. Application of the Archimedes' principle leads to the following expression for the density ( $\rho_{mmc}$ ) of the composites:

$$\rho_{mmc} = \frac{m}{m - m_1} \rho_w, \quad (1)$$

where  $m$  is the mass of the composite sample in air,  $m_1$  is the mass of the same composite sample in distilled water and  $\rho_w$  is the density of the distilled water. The density of distilled water at 20 °C is 998 kg/m<sup>3</sup>. Using this method, the densities of the base metal and hybrid composites were measured.

During the process of fabrication of MMCs, some porosity levels are normal, because of the long particle feeding and the increase in surface area in contact with air. The volume fraction of porosity, its size and distribution in a cast MMCs play an important role in controlling the mechanical properties. Porosity levels must, therefore, be kept to a minimum. Porosity cannot be fully avoided during the casting process, but it can, however, be controlled. Porosity of the composites was estimated by the following equation:

$$\text{Porosity} = \frac{\rho_{th} - \rho_m}{\rho_{th}} \quad (2)$$

where  $\rho_{th}$  and  $\rho_m$  are the theoretical and measured densities, respectively.  $\rho_{th}$  for a single constituent can be found from the rule of mixtures.

$$\rho_{th} = \rho_m V_m + \rho_r V_r \quad (3)$$

where  $\rho_m$  is the density of the matrix,  $V_m$  is the volume fraction of matrix,  $\rho_r$  is the density of reinforcement and  $V_r$  is the volume fraction of reinforcement.

The empirical relation for density can be modified for hybrid composites, by including the volume fractions for both the reinforcements (RHA and SiC) as follows:

$$\rho_{th} = \rho_{Al} V_{Al} + \rho_{RHA} V_{RHA} + \rho_{SiC} V_{SiC} \quad (4)$$

where  $\rho_{Al}$ ,  $\rho_{RHA}$ ,  $\rho_{SiC}$  are the densities of aluminum alloy, rice husk ash and SiC, respectively;  $V_{Al}$ ,  $V_{RHA}$ ,  $V_{SiC}$  are the volume fractions of aluminum alloy, rice husk ash and SiC, respectively. Also

$$V_{Al} = 1 - (V_{RHA} + V_{SiC}) \quad (5)$$

The volume fraction of the reinforcement was calculated from Eq. (6)

$$V_r = \frac{\rho_m - \rho_{mmc}}{\rho_m - \rho_r} \quad (6)$$

## 2.7. Mechanical behavior

Tensile testing of the extruded samples was conducted in accordance with the ASTM E8 standard on round tension test specimens of diameter 10 mm and gauge length 60 mm using an automated servo-hydraulic testing machine (Instron 8501), with cross-head speed set at 0.254 mm/min. An initial strain rate of  $1.69 \times 10^{-4} \text{ s}^{-1}$  was used. The experiments were conducted at room temperature.

## 2.8. Age hardening studies of hybrid composites

Brinell hardness measurements were used to ascertain the age hardening behavior of the composites in the present study. The aging temperature was maintained at 155 °C for different time intervals. The composites subjected to aging were tested for their hardness using a Brinell hardness tester. A test load of 500 kg is applied to the specimens for 30 s. The diameter of the steel ball indenter was 10 mm. The size of the indent ( $d$ ) was determined optically by measuring two diagonals of the round indent. The Brinell hardness number (BHN) was calculated for the unreinforced and hybrid composites using Eq. (7). An average of five readings was taken for each sample for hardness measurement.

$$\text{BHN} = \frac{2F}{\pi D(D - \sqrt{D^2 - d^2})} \quad (7)$$

where  $F$  is the applied load in kg,  $D$  is the diameter of the steel ball in mm and  $d$  is the size of the indent in mm. Each hardness value presented is an average of at least five symmetrical indentations.

# 3. Results and discussion

## 3.1. Microstructural characterization

Fig. 1a and b shows the scanning electron micrographs of RHA and SiC sample. It could be observed that the rice husk ash consists of particulates with different sizes and different shapes. The average sizes of the rice husk ash and SiC

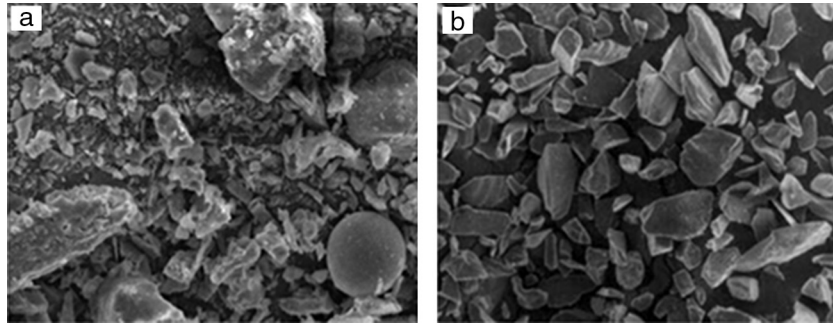


Fig. 1 – Scanning electron micrographs of (a) rice husk ash sample and (b) SiC particulates.

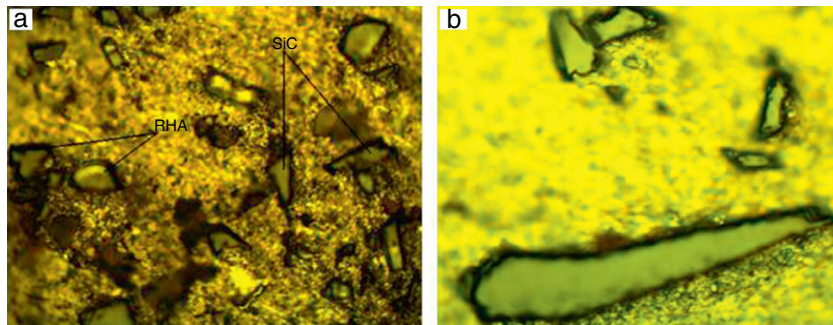


Fig. 2 – Optical micrograph (a) hybrid composite and (b) at the interface.

samples were found to be  $25\ \mu\text{m}$  and  $35\ \mu\text{m}$ , respectively. The optical micrographs of aluminum composites reinforced with RHA and SiCp are shown in Fig. 2a and b. Optical micrographs of hybrid composites show clearly the uniform distribution of RHA and SiC in the matrix, and no void and discontinuities were observed. There was a good interfacial bonding between the particles and matrix material (Fig. 2b). Fig. 3 shows the scanning electron micrograph of the hybrid composite.

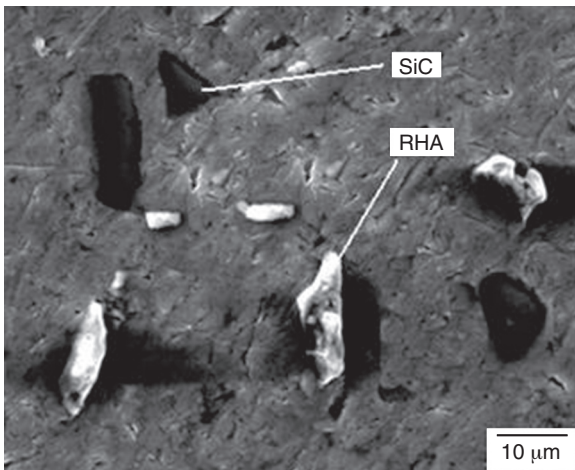


Fig. 3 – Scanning electron micrograph of Al/RHA/SiC hybrid composite.

### 3.2. XRD characterization

The XRD pattern of the purified rice husk ash sample is shown in Fig. 4. Only peaks corresponding to silicon dioxide and graphite are observed for RHA. The ash contains fixed carbon which does not burn off even at  $1000^\circ\text{C}$ .

### 3.3. Density and porosity measurements

Fig. 5 shows the variation in measured density and the porosity of the base metal and the hybrid composites. It could be observed that the density decreases with increase in the reinforcement. The decrease in densities of the hybrid composites was due to the presence of low density RHA particulates. The theoretical densities are obtained from the rule of mixtures using Eqs. (1)–(7). Based on the measured and theoretical densities the porosity of aluminum alloy and the hybrid composites was measured and found to increase with the increase in reinforcement, as shown in Fig. 5. The increase in porosity can be attributed to gas entrapment during mixing, hydrogen evolution, shrinkage during solidification, and air bubbles entering the slurry either independently or as an air envelope to the reinforcement particles.

### 3.4. Mechanical behavior

The results of the tensile tests at room temperature are shown in Fig. 6 with the weight % of reinforcement particles. From the figure it is observed that the ultimate tensile strength (UTS) and yield strength (YS) increase with an increase in the percent

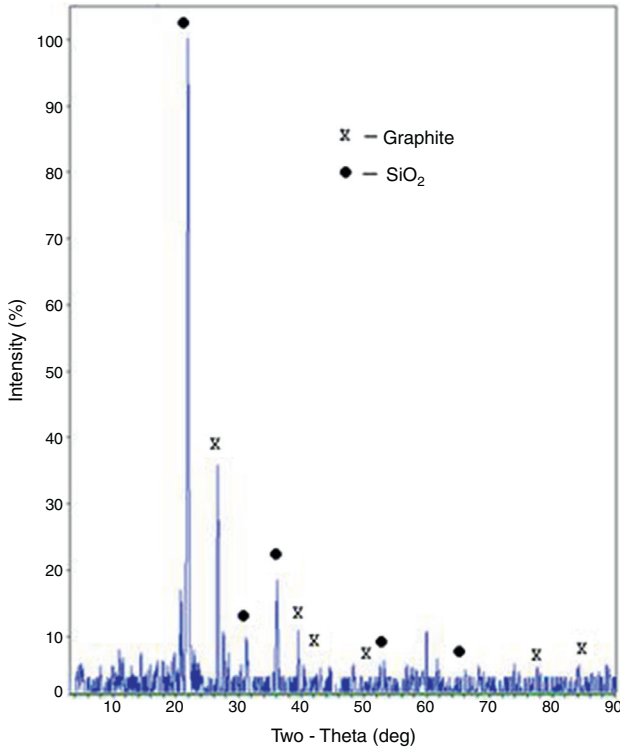


Fig. 4 – XRD pattern for RHA.

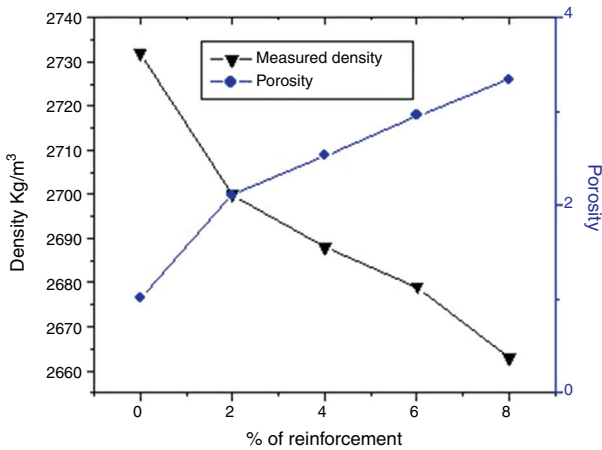


Fig. 5 – Variation in density and porosity with % reinforcement.

weight fraction of reinforcement particles and % elongation decreases with the increase in weight % of reinforcement particles. Higher the particle content, lower the elongation due

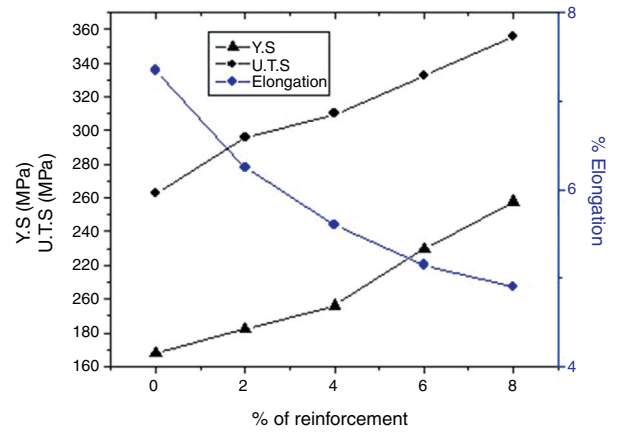


Fig. 6 – Variation in yield strength, ultimate tensile strength and elongation with % reinforcement.

to the increase in UTS and YS. The corresponding values are presented in Table 3.

Several theories and mechanisms have been suggested to explain the strengthening of MMCs. However, the strength of the composites does not depend on a unique mechanism but several mechanisms may act simultaneously. In the present study, strengthening effect is mainly through an increased dislocation density arising from a thermal mismatch between the matrix and reinforcement.

Metal matrix composites are characterized by a large difference in the thermal expansion coefficient (CTE) of the matrix and the reinforcement (CTE of A356.2 is  $21.4 \times 10^{-6}/^{\circ}\text{C}$ , the CTE of RHA is  $10.1 \times 10^{-6}/^{\circ}\text{C}$  and the CTE of SiC is  $4.3 \times 10^{-6}/^{\circ}\text{C}$ ). Even small temperature changes generate thermal stresses in the aluminum matrix. These stresses can be partially released by dislocation generation in the vicinity of the interface. Thus the dislocation density generated can be quite significant at the interface and can be predicted using the model of Taya and Arsenault [12] based on prismatic punching of dislocations at a ceramic particulate. The dislocation density  $\rho$  at the interface is given by Eq. (8)

$$\rho = \frac{B\varepsilon V_f}{bd(1 - V_f)} \tag{8}$$

The empirical relation for dislocation density can be modified for hybrid composites as

$$\rho = \frac{B\varepsilon(V_{RHA} + V_{SiC})}{bd(1 - (V_{RHA} + V_{SiC}))} \tag{9}$$

Table 3 – Mechanical properties of matrix and hybrid composites.

S.no.	Sample	Hardness BHN	YS MPa	UTS MPa	% elongation
1	A356.2 alloy	68	168	263	7.35
2	A356.2/2%RHA/2%SiC hybrid composite	74	182	296	6.25
3	A356.2/4%RHA/4%SiC hybrid composite	83	196	310	5.6
4	A356.2/6%RHA/6%SiC hybrid composite	96	230	333	5.15
5	A356.2/8%RHA/8%SiC hybrid composite	104	258	356	4.9

where  $B$  is a geometric constant that depends on the aspect ratio (it varies between 12 for equiaxed particulate and 4 for whisker-like particulate),  $\varepsilon$  is the thermal mismatch strain (the product of temperature change  $\Delta T$ , during solidification of MMCs and CTE difference,  $\Delta\alpha$ , between reinforcement and matrix),  $V_r$  is the volume fraction of the reinforcement,  $b$  is the Burgers vector, and  $d$  is the average grain diameter of reinforcements.

The CTE of the composites is relatively difficult to predict because it is influenced by several factors such as the internal structure of the composite, plasticity, etc. However, there are several analytical methods to predict CTE of the composites, which include simple rule of mixtures and thermo-elastic energy principles such as Kerner and Turner models. Based on the Kerner model, the CTE of the composites can be predicted using the following equation

$$\alpha_C = \alpha_p V_p + \alpha_m V_m + (\alpha_p - \alpha_m) V_p V_m \times \frac{K_p - K_m}{V_p K_p + V_m K_m + 3/4 K_p K_m L_m} \quad (10)$$

Based on the Turner model, the CTE of the composites can be predicted using the following equation

$$\alpha_C = \frac{\alpha_p V_p K_p + \alpha_m V_m K_m}{V_p K_p + V_m K_m} \quad (11)$$

where  $V$  is the volume fraction and  $\alpha$  the CTE of the component. The subscripts  $c$ ,  $p$ , and  $m$  refer to the composite, particle and matrix, respectively.  $K$  is the bulk modulus of the components of the composite which can be found from the simple relations between elastic constants.

And based on the rule of mixtures (ROM), the CTE of the composites is given by

$$\alpha_C = \alpha_p V_p + \alpha_m V_m \quad (12)$$

The CTE of the hybrid composites is given by

$$\alpha_c = \alpha_m V_m + \alpha_{RHA} V_{RHA} + \alpha_{sic} V_{sic} \quad (13)$$

Based on the above equations it was also observed that the CTE decreases and the dislocation density increases with the increase in percentage of reinforcement, as shown in Fig. 7. The dislocation densities for the hybrid composites were then calculated based on equation 9 with an assumption for the Burgers vector of 0.32 nm for Al [6], and are tabulated in Table 4. The dislocation arrangement in the hybrid composites is shown in Fig. 8.

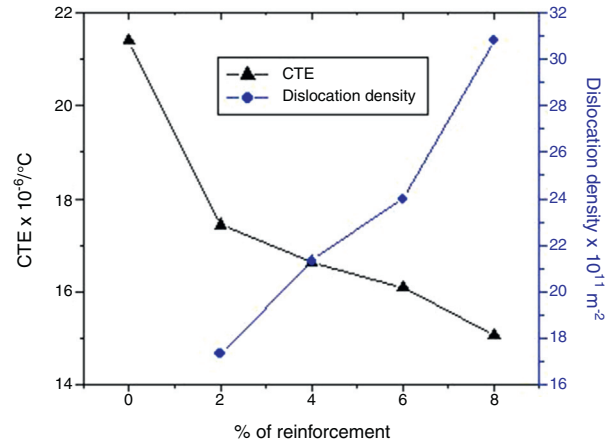


Fig. 7 – Variation in CTE and dislocation density with % reinforcement.

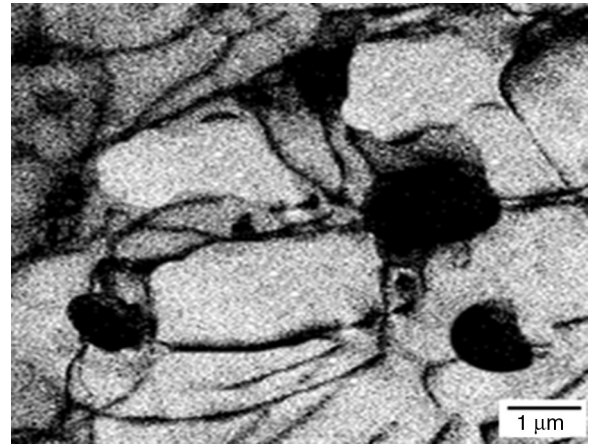


Fig. 8 – The dislocation arrangement in the hybrid composites.

For the strengthening due to the presence of dislocations generated by the differential CTE, the following equation may be used:

$$\Delta\sigma_T = \alpha G b (\rho)^{1/2} \quad (14)$$

where  $\Delta\sigma_T$  is the yield strength contribution due to geometrical necessary dislocations,  $\alpha$  is a constant (values 0.5–1),  $G$  is the shear modulus, and  $b$  is the Burger vector. The reinforcing phase contributes to strengthening mainly through an increased dislocation density arising from thermal mismatch.

Table 4 – Theoretical results of unreinforced and hybrid composites.

S.no.	Weight (%) of reinforcement	Estimated dislocation density, $\rho$ ( $\text{m}^{-2}$ )	CTE, $\alpha$ ( $^{\circ}\text{C}$ )
1	0.0	–	$21.4 \times 10^{-6}$
2	2.0	$17.31 \times 10^{11}$	$17.44 \times 10^{-6}$
3	4.0	$21.32 \times 10^{11}$	$16.64 \times 10^{-6}$
4	6.0	$23.99 \times 10^{11}$	$16.09 \times 10^{-6}$
5	8.0	$30.82 \times 10^{11}$	$15.06 \times 10^{-6}$

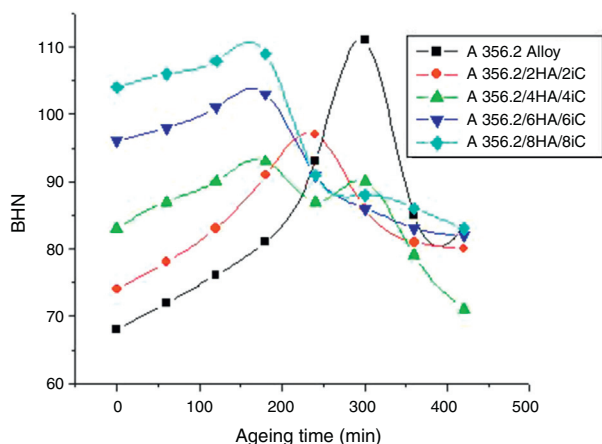


**Fig. 9 – Brinell hardness versus the aging time for the alloy and hybrid composites.**

### 3.5. Aging studies of A356.2/RHA/SiC hybrid composites

The aging response of the A356.2/RHA/SiC hybrid composites at a temperature of 155 °C was studied. Fig. 9 shows the effect of aging time on the hardness of reinforced and unreinforced A356.2 alloy. It could be observed that, an increase in the hardness of the composite materials occurred after the aging treatment. However, it is of interest to note that peak hardness was observed at lower aging times for the hybrid composite compared to that of the Al base alloy (240 min for the A356.2/2%RHA/2%SiC hybrid composite, 180 min for A356.2/4%RHA/4%SiC, A356.2/6%RHA/6%SiC, A356.2/8%RHA/8%SiC hybrid composites and 300 min for the Al alloy). These results indicate that the addition of reinforcement to the aluminum matrix accelerates the aging kinetics. This behavior can be related to the high matrix dislocation density induced by the thermal mismatch between the matrix and the reinforcement. It is well known that high dislocation density in the metal matrix promotes dislocation-assisted diffusion of the aging elements.

## 4. Conclusions

From this study the following conclusions are drawn:

- Hybrid metal matrix composites with up to 8% rice hush ash and SiC particles could be easily fabricated using double stir casting process.
- Uniform distribution of rice husk ash and SiC was observed in the matrix.
- The density of hybrid composites decreases, whereas the porosity and hardness increases with the increase in percentage of the reinforcement.
- The CTE of the hybrid composites decreases with the increase in percentage of the reinforcement.

- The yield strength and ultimate tensile strength increase with the increase in RHA and SiC content. The strength improvement of hybrid composites can be attributed to the increase in the dislocation density.
- It was found that in comparison to that of base aluminum alloy, the precipitation kinetics were accelerated by adding the reinforcement. This effect reduced the time for obtaining the maximum hardness by the aging heat treatment. The reason for the improvement is related to the higher dislocation density of the metal matrix, due to the thermal mismatch.

## Conflicts of Interest

The authors declare no conflicts of interest.

## REFERENCES

- [1] Mahendra KV, Radha Krishna K. Characterization of Stir Cast Al-Cu-(fly ash + SiC) hybrid metal matrix composites. *Journal of Composite Materials* 2010;44(8):989–1005.
- [2] Siva Prasad D, Rama Krishna A. Production and mechanical properties of A356.2/RHA composites. *International Journal of Advanced Science and Technology* 2011;33:51–7.
- [3] Ramachandra M, Radhakrishna K. Synthesis-microstructure-mechanical properties-wear and corrosion behavior of an Al-Si (12%) – Flyash metal matrix composite. *Journal of Materials Science* 2005;40:5989–97.
- [4] Sanjeev Das, Udhayabanu V, Das S, Das K. Synthesis and characterization of zircon/Al–4.5%Cu composite produced by stir casting route. *Journal of Materials Science* 2006;41:4668–77.
- [5] Siva Prasad D, Rama Krishna A. Tribological properties of A356.2/RHA composites. *Journal of Materials Science and Technology* 2012;28(4):367–72.
- [6] Siva Prasad D, Rama Krishna A. Effect of heat treatment on the damping behavior of A356.2/RHA composites. *Bulletin of Material Science* 2012;35(6):989–95.
- [7] Suresha S, Sridhara BK. Wear characteristics of hybrid aluminium matrix composites reinforced with graphite and silicon carbide particulates. *Composites Science and Technology* 2010;70:1652–9.
- [8] Leng J, Jiang L, Gaohui Wu QZ, Sun D, Zhou Q. Study of machinable SiC/Gr/Al composites. *Journal of Material Science* 2008;43:6495–9.
- [9] Alanemea KK, Akintund IB, Olubamb PA, Adewal TM. Fabrication characteristics and mechanical behaviour of rice husk ash – alumina reinforced Al–Mg–Si alloy matrix hybrid composites. *Journal of Materials Research and Technology* 2013;2(1):60–7.
- [10] Mishra P, Chakraverty A, Banerjee HD. Production and purification of silicon by calcium reduction of rice-husk white ash. *Journal of Materials Science* 1995;20:4387–91.
- [11] Rodriguez de Sensale G. Strength development of concrete with rice husk ash. *Cement and Concrete Composites* 2006;28:158–60.
- [12] Taya M, Arsenault RJ. *Metal matrix composites—thermomechanical behavior*. New York, USA: Pergamon Publishers; 1989.